Int. J. Oral Maxillofac. Surg. 2019; 48: 309–321
https://doi.org/10.1016/j.ijom.2018.10.013, available online at https://www.sciencedirect.com

International Journal of Oral & Maxillofacial Surgery

Research Paper
Craniofacial Anomalies

Orbit, zygoma, and maxilla growth patterns in Crouzon syndrome

X. Lu[1], A. J. Forte[2], R. Sawh-Martinez[3], R. Wu[3], R. Cabrejo[3], D. M. Steinbacher[3], M. Alperovich[3], N. Alonso[4], J. A. Persing[3]

[1]Chinese Academy of Medical Sciences, Peking Union Medical College, Plastic Surgery Hospital, Beijing, China; [2]Division of Plastic and Reconstructive Surgery, Mayo Clinic Florida, Jacksonville, Florida, USA; [3]Section of Plastic and Reconstructive Surgery, Yale School of Medicine, New Haven, Connecticut, USA; [4]Department of Plastic Surgery, University of São Paulo, São Paulo, Brazil

X. Lu, A. J. Forte, R. Sawh-Martinez, R. Wu, R. Cabrejo, D. M. Steinbacher, M. Alperovich, N. Alonso, J. A. Persing: Orbit, zygoma, and maxilla growth patterns in Crouzon syndrome. Int. J. Oral Maxillofac. Surg. 2019; 48: 309–321. © 2018 International Association of Oral and Maxillofacial Surgeons. Published by Elsevier Ltd. All rights reserved.

Abstract. The facial malformations of Crouzon syndrome involve the entire cranio-orbito-zygomatic region. The detailed sequence of changes in orbit, zygoma, and maxilla over time, the mutual influence among these three anatomical structures, and their relationship with the cranial base were studied to determine the sequence and timing of deformity. Preoperative CT scans of 36 patients with Crouzon syndrome (mean age 10.84 ± 14.70 years; 14 male, 22 female) and CT scans of 54 control subjects (mean age 8.53 ± 13.22 years; 29 male, 25 female) were divided into five subgroups by age: 0–6 months, 6 months–2 years, 2–6 years, 6–18 years, and 18–62 years. Craniofacial morphometric cephalometrics were analyzed using Materialise software. Crouzon orbit anteroposterior length was shorter before 6 months ($P = 0.021$) and remained shorter into adulthood ($P < 0.001$). Globe projection was greater across all age subgroups ($P < 0.001$), reaching a peak at 6 months to 2 years ($P < 0.001$). The increased medial orbital width was the most remarkable and persistent secondary deformity ($P < 0.001$). The zygoma anterior protrusion was retruded before 6 months of age ($P < 0.001$), but then improved gradually. The width of maxilla was greater by 24% in the Crouzon cohort ($P < 0.001$), with a difference of 16% before 6 months ($P = 0.024$), and was developed earlier than the shortened anteroposterior length. Crouzon high and shallow orbital walls are distinctive. Maxillary widening developed before the malformation of sphenoid. The anteroposterior position of zygoma is likely a principal deformity, rather than a reflection of the intrinsic shape of the bone.

Level of Evidence: II

Key words: Crouzon syndrome; orbit; zygoma; maxilla; midface.

Accepted Available online 30 October 2018
Available online 30 October 2018

The characteristic facial malformations of Crouzon syndrome, like orbital deformity and midface retrusion, involve the entire cranio-orbito-zygomatic region[1–3]. Visual impairments, such as strabismus and ametropia, caused by the deformed orbital bony structure, are universal and associated with exorbitism[4,5]. These orbital symptoms are more severe in Crouzon syndrome compared with Apert syndrome, which shares a similar fibroblast growth factor 2 (FGF-2) activating muta-

 © 2018 International Association of Oral and Maxillofacial Surgeons. Published by Elsevier Ltd. All rights reserved.

tion[6]. Kreiborg and Cohen speculated that this may be due to their different pathogeneses[7]. The shallower orbital cone and shorter orbital walls in Crouzon syndrome could be the primary influence of skeletal development, while Apert deformities may be due to cranial base dysmorphology[7]. Exorbitism could also be caused by the disharmonious globe–orbit relationship, with increased globe prominence but decreased bony orbit volume[8,9].

Among the six bones comprising the bony orbit, the zygoma contributes a considerable proportion. It has significant overall influence on orbital appearance as well as the shape, size, and direction of the entire orbit. With the exception of the nose, the zygoma is the most prominent aspect in the midface, and helps determine the facial width, its lateral curvature, and sex-specific characteristics[10]. Taken together, there is a delicate interplay between the orbit, zygoma, and maxilla, in which changes in one may be caused by, or in turn, affected by, changes in the others[11].

Previous studies have shown that the development of facial abnormality is synchronized with cranial base malformation[12]. The facial deformity begins in the anterior cranial base-related orbital zone and then progresses to the middle cranial base-related area, with the most severe deformity manifesting in the midface. However, in light of this metachronous development, the question may be asked, what are the detailed changes of these three anatomical segments?

The purpose of this study was to objectively analyze the morphological and spatial changes of orbit, zygoma, and maxilla over time in a series of unoperated patients with Crouzon syndrome compared to controls. An additional aim was to determine the relationship and mutual influence among these three anatomical regions and the cranial base.

Patients and methods

This longitudinal study was performed in accordance with the requirements of the Institutional Human Investigation Committee at Yale University. Computed tomography (CT) scans were obtained for all subjects, none of whom had undergone any previous surgical intervention. Preoperative CT scans were obtained from 36 patients with Crouzon syndrome and 54 control subjects without any confounding disease; controls were age- and sex-matched to Crouzon patients. The CT scans were divided into five subgroups based on age: 0–6 months, 6 months–2 years, 2–6 years, 6–18 years, 18–62 years. Age and sex were re-matched in each age subgroup to confirm comparability. Demographic information was tabulated.

Digital Imaging and Communications in Medicine (DICOM) data were digitized and measured using Mimics version 19.0 and 3-matics version 11.0 software (both Materialise, Leuven, Belgium). The entire package of abbreviations and definitions of measurements are reported in Tables 1–3.

Additionally, some unique measurements were designed and included in this study: (1) zygoma transverse width, defined as the distance between the zygomatic 'peak point' and the self-base plane. The self-base plane was produced by the three midpoints of the three sutures around zygoma: the zygomaticomaxillary suture, zygomaticotemporal suture, and zygomaticofrontal suture. The zygomatic peak point was produced by the 'create part comparison analysis' function in 3-matics software (Fig. 1). (2) The zygoma anterior protrusion, defined as the distance from the most anterior point of zygoma to the rear base plane, which passed through sella and was simultaneously perpendicular to the Frankfort horizontal plane and the median sagittal plane (Fig. 2). (3) The frontozygomatic suture length, defined as the distance between the most anterior point of pterion and the frontozygomatic suture point; the projected length of the frontozygomatic suture length is its effective length in the Frankfort horizontal plane. The rotated angle of the line con-

Table 1. Definitions of landmarks.

Variable	Abbreviation	Definition
Nasal aperture point	ALR/ALL	The most lateral and inferior points of the nasal aperture in a transverse plane
Anterior nasal spine	ANS	The tip of the median, sharp bony process of the maxilla at the lower margin of the anterior nasal opening
Corneae	Cornea R/L	The most anterior point of cornea
Frontozygomatic point	FZR/FZL	The most medial and anterior point of each frontozygomatic suture at the level of the lateral orbital rim
Medial orbital point	MOR/MOL	The most medial point of the bony orbit
Nasion	N	The junction of the frontonasal suture at the most posterior point on the curve at the bridge of the nose
Nasal cavity point	NcR/NcL	Nasal cavity widest points
Optic foramen point	OFR/OFL	The midpoint of the rim of optic foramen
Orbitale	ORR/ORL	The most inferior point of each infraorbital rim
Pterion point	PR/PL	The most anterior point of pterion
Medial pterygoid plate	PP	The most anterior point of the medial pterygoid plate at the pterygomaxillary fissure
Lateral pterygoid plate	PPR/PPL	The most lateral point of the most inferior portion of the lateral pterygoid plate
Rhinion	Ro	The anterior tip at the end of the suture of the nasal bones
Sella	S	The center of the hypophyseal fossa (sella turcica)
Orbital uppermost point	UORR/UORL	The uppermost points on the roof of the orbit
Zygomaticomaxillary suture point	ZMR/ZML	The point at the zygomaticomaxillary suture on the anterior margin of the inferior orbital rim on each side
Zygoma peak point	ZPR/ZPL	The furthest point to the zygomatic self-base plane. The self-base plane was produced from the three midpoints of the three sutures around zygoma: the zygomaticomaxillary suture, zygomaticotemporal suture, and zygomaticofrontal suture
Zygomaticotemporal suture point	ZTR/ZTL	The midpoint of the zygomaticotemporal suture
Zygomatic lowest point	ZXR/ZXL	The lowest point of zygoma
Zygion	ZYR/ZYL	The most lateral point on the outline of each zygomatic arch

R, right; L, left.

Table 2. Definitions of cephalometric distances, ratios, and angles of the orbit.

Variable	Definition
Unilateral orbital features	
Orbit length	The distance from the zygomaticomaxillary suture on the orbital rim to the optic foramen
Orbit height	The distance between the mid-superior and mid-inferior orbital rim on a sagittal plane crossing the corneal apex
Orbit width	The distance between the most anterior portion of the medial and the lateral orbital walls on an axial plane crossing the corneal apex
Vertical cone angle	Angulation of the vertical walls of the posterior orbit as defined by three points: the superior-most point of the orbital roof, vertex at the optic foramen, and inferior point on the orbital floor in the same sagittal slice as the superior point
Inner horizontal cone angle	The angle was measured on the plane passing through the midpoint of bilateral corneae and parallel to the FH plane; the vertex is at the optic foramen and the other two points are the midpoint of the lateral orbital wall and the medial point of the ethmoid bone
External horizontal cone angle	The angle was measured on the plane passing through the midpoint of bilateral corneae and parallel to the FH plane; the vertex is at the optic foramen and the other two points are the anterior-most point of the lateral orbital wall and the medial point of the ethmoid bone
Orbital rim angle	The angle of the orbital rim plane to the middle sagittal plane. The orbital rim plane was defined by points on the orbital rim: supraorbital notch, zygomaticofrontal suture, and zygomaticomaxillary suture
Globe projection	The distance from the most anterior point of cornea to the orbital rim plane
Visual axis length	The distance between the cornea and optic foramen
Visual axis length/orbit length	The ratio of the distance between the cornea and optic foramen to the distance from the zygomaticomaxillary suture on the orbital rim to optic foramen
Bilateral orbital relationship	
Medial orbital width (MOR–MOL)	The distance between bilateral points on the medial orbital margin that is closest to the median plane
Interzygomaticofrontal suture distance (FZR–FZL)	The distance between bilateral zygomaticofrontal sutures (point along the orbital rim)
Upper orbital width (UORR–UORL)	The distance between bilateral uppermost points on the roof of the orbit, representing the upper face breadth
Orbitale width (ORR–ORL)	The distance between the bilateral lowest points on each infraorbital rim
Optic foramen distance (OFR–OFL)	The distance between bilateral optic foramen points
Corneae distance	The distance between bilateral corneae
Bilateral optical axis angle	The angle between bilateral optical axis lines; the line was defined as connecting optic foramen and corneae

FH, Frankfort horizontal.

necting pterion and the frontozygomatic point is the angle between the line and Frankfort horizontal plane (Fig. 3). These measurements were designed to describe the detailed morphology of the pterion area.

Before the initial data acquisition for this study, the observer underwent measurement training until the inter-observer Pearson correlation coefficient (compared with a practiced observer) was $\geq$0.95 and the intra-observer error was <0.05. All landmark points, generated lines, angles, and planes were selected and produced twice by the same observer, in both the Crouzon syndrome and control group, with independent verification by two additional observers (plastic surgeons).

Statistical analyses

The *t*-test was used for the analysis of continuous variables (Microsoft Excel, v.2016; Microsoft Corp., Redmond, WA, USA). The Pearson correlation coefficient was calculated to evaluate inter-observer and intra-observer correlations (IBM SPSS Statistics, version 24.0; IBM Corp., Armonk, NY, USA). All statistical tests were two-tailed and statistical significance was set at $P < 0.05$.

Demographic data

Ninety CT scans were included (Crouzon, $n = 36$; control, $n = 54$). The five age subgroups were 0–6 months, 6 months–2 years, 2–6 years, 6–18 years, and 18–62 years. The mean age of the Crouzon group subjects was 10.84 $\pm$ 14.70 years (range 3 days to 62 years) and the mean age of the control group subjects was 8.53 $\pm$ 13.22 years (range 5 days to 62 years). The Crouzon group consisted of 14 males and 22 females and the control group of 29 males and 25 females (Table 4).

Results

Unilateral orbital features

Prior to 6 months of age, the anteroposterior bony orbit length was significantly shorter by 13% in the Crouzon group compared to controls ($P = 0.021$) and remained shorter, by at least 20%, into adulthood ($P < 0.001$). Orbital height was initially greater than in controls (21% before 6 months of age; $P < 0.001$) and remained increased into adulthood (17%, $P < 0.001$) (Fig. 4). The orbital width did not differ significantly between Crouzon patients and controls across all time points.

The vertical cone angle was more obtuse in Crouzon patients after 2 years of age. Although the inner horizontal cone angle paralleled the development of controls, the external horizontal cone angle of Crouzon patients was significantly greater after 6 years of age (Fig. 5). The orbital rim angle decreased 6% compared with controls ($P < 0.001$). Globe projection was greater in the Crouzon cohort across all age subgroups, by 139% on average ($P < 0.001$), reaching a peak at 6 months to 2 years (185% increase compared with controls; $P < 0.001$) (Fig. 6). The ratio of the visual axis to bony orbital length correspondingly increased by 28% compared to controls ($P < 0.001$) (Tables 5 and 6).

Table 3. Definitions of cephalometric distances and angles of zygoma and midface, and related cranial base measurements.

Variable	Definition
Zygomatic linear measurements	
Zygoma anterior protrusion	The distance from the most anterior point of zygoma to the plane representing the most anterior of the frontal bone
Zygoma self-protrusion	The distance between the zygomatic peak point and self-base plane. The self-base plane was produced by the three midpoints of the three sutures around zygoma: the zygomaticomaxillary suture, zygomaticotemporal suture, and zygomaticofrontal suture
Zygoma height	The distance from the most superior point on zygoma to the most inferior point on zygoma
Zygoma length	The distance from the midpoint of the zygomaticomaxillary suture to the midpoint of the zygomaticotemporal suture
Zygoma superior curvature length	The distance from the most superior anterior point on the zygomaticofrontal suture (point along the orbital rim) to the most anteromedial point on the zygomaticomaxillary suture (point along the orbital rim)
Bizygomatic width (ZYR–ZYL)	The distance between the bilateral most lateral point on the outline of each zygomatic arch
Frontozygomatic suture length (PR/L–FZR/L)	The distance between the most anterior point of pterion and the frontozygomatic suture point; suggests the length of the frontozygomatic suture
Projected length of pterion–FZR/L	The effective length of pterion–FZR/L in the FH plane
Rotated angle of pterion–FZR/L	The angle between the line of pterion–FZR/L and the FH plane
Geometry of zygoma	
Fronto-orbital zygomatic angle (UORR/L–FZR/L–ORR/L)	The vertex at the frontozygomatic point and the other two points – the highest point of the orbital rim and the lowest one on the same side
Zygomaticosphenoid angle (ZMR/L–FZR/L–ZTR/L)	The vertex at the frontozygomatic point and the other two points – the zygomaticomaxillary suture point and the zygomaticotemporal suture point
Frontal zygomatic angle (ZMR/L–ZPR/L–ZTR/L)	The vertex at the zygoma peak point and the other two points – the zygomaticomaxillary suture point and the zygomaticotemporal suture point
Zygoma anterior angle (ZMR/L–ZPR/L–FZR/L)	The vertex at the zygoma peak point and the other two points – the zygomaticomaxillary suture point and the frontozygomatic point
Zygoma vertical angle (FZR/L–ZPR/L–ZXR/L)	The vertex at the zygoma peak point and the other two points – the frontozygomatic point and the zygomatic lowest point
Midface	
Maxillary width (ZMR–ZML)	The distance between bilateral zygomaticomaxillary suture points
Maxillary length (ANS–PP)	The distance between anterior nasal spine and medial pterygoid plate
Nasal base width (ALR–ALL)	The distance between the most lateral and inferior points of the nasal aperture in a transverse plane
Nasal width (NcR–NcL)	The distance between bilateral nasal cavity widest points
Nasal base height (Ro–ANS)	The distance between rhinion and anterior nasal spine; indicates the height of midface
Nasal length (N–Ro)	The distance between nasion and rhinion; indicates the height of midface
Related cranial base measurements	
Sphenoid greater wing angle	Measured from the plane passing through the midpoint of the bilateral most in-front points of corneae and parallel to FH plane; indicates the sphenoid greater wing divergence
PPR–S–PPL	The angle between bilateral lateral pterygoid plates, measured by connecting points PPR, S, and PPL; indicates the separation of lateral pterygoid
N–S–PP	Corresponding to the degree of backward rotation of the pterygoid plates

FH, Frankfort horizontal.

Bilateral orbital relationship

The increasing medial orbital width (MOR–MOL) was the most remarkable and persistent; this was 13% wider in Crouzon subjects before 6 months of age ($P = 0.043$), and they experienced an average increase of 24% throughout life ($P < 0.001$). The lateral orbital width (the distance between zygomaticofrontal sutures (FZR–FZL)) was longer by 9% on average in all age groups ($P = 0.009$). Whole group comparisons found that Crouzon subjects had significantly increased upper orbital width (UORR–UORL), orbitale width (ORR–ORL), and distance between bilateral optic foramen (OFR–OFL) by 23% ($P < 0.001$), 19% ($P < 0.001$), and 11% ($P = 0.037$), respectively, reflective of ethmoid sinus expansion. The soft tissue developed corresponding changes. The bilateral corneal distance was significantly greater in Crouzon compared with controls in the whole group analysis (23%, $P < 0.001$), with a consequently increased bilateral optical axis angle (30%, $P < 0.001$).

Zygomatic linear measurements

The zygoma anterior protrusion was strikingly retruded by 104% ($P < 0.001$) in Crouzon compared with controls ($P < 0.001$) prior to 6 months. This was followed by a gradual improvement to a 27% reduction by adulthood. The zygoma transverse width, however, was not different between Crouzon patients and controls. The Crouzon zygoma height was 15% ($P = 0.018$) shorter when compared with controls at 6 months to 2 years of age, and zygoma length was shorter in all age

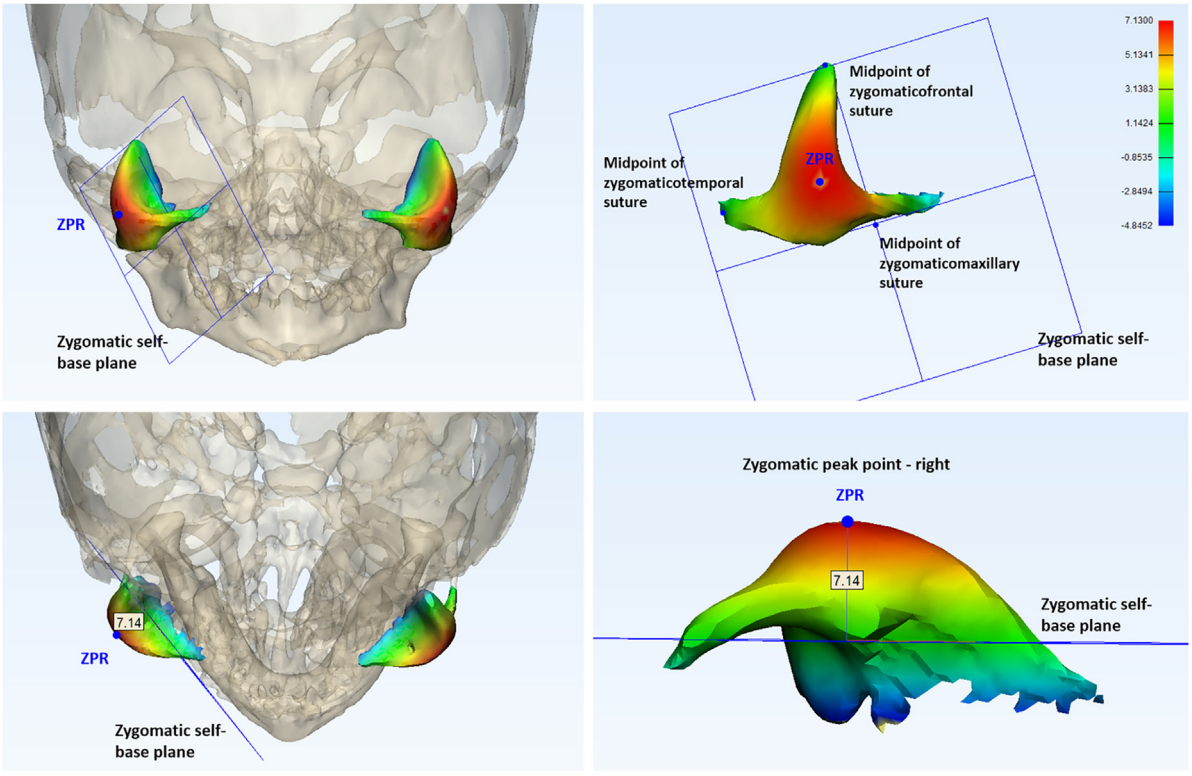

Fig. 1. The zygoma transverse width was measured as the distance between the zygomatic peak point and self-base plane. The self-base plane was produced by the three midpoints of the three sutures around zygoma: the zygomaticomaxillary suture, zygomaticotemporal suture, and zygomaticofrontal suture. The zygomatic peak point was produced by the 'create part comparison analysis' function bar in 3-matics software (version 11.0; Materialise, Leuven, Belgium).

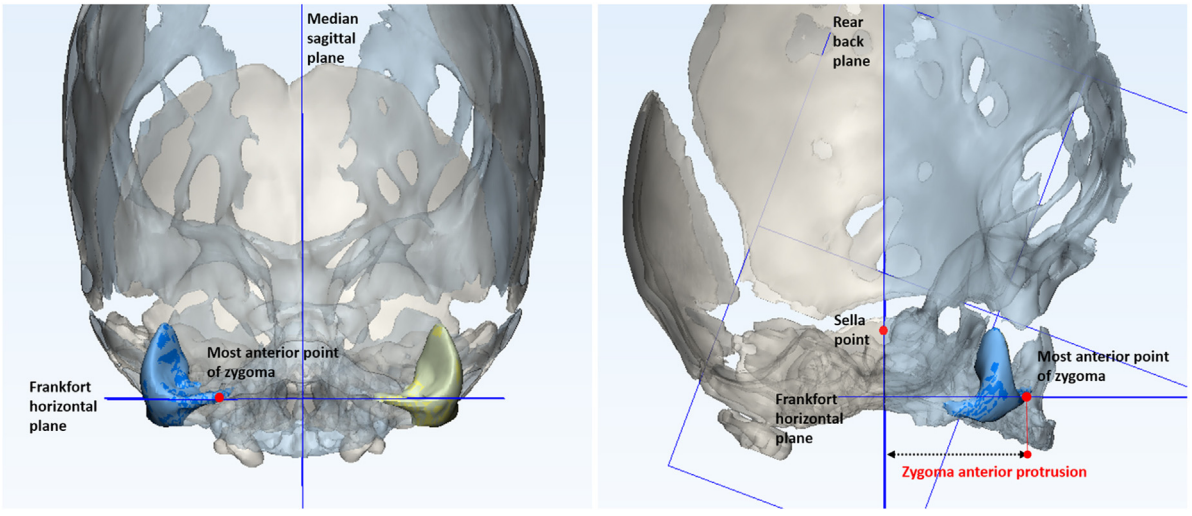

Fig. 2. The zygoma anterior protrusion was measured as the distance between the most anterior point of zygoma and the rear base plane, which passes through the midpoint of sella and is simultaneously perpendicular to the Frankfort horizontal plane and median sagittal plane.

groups following 6 months, by at least 12%. While the zygoma superior curvature length was increased by 8% ($P = 0.046$) in adult Crouzon subjects, the bizygomatic width was normal throughout growth (Tables 5 and 7).

Prior to 6 months of age, the distance between pterion and the frontozygomatic suture point (pterion–FZR/L), indicting the length of the sphenofrontal suture, was decreased by 3.63 mm (20%, $P = 0.018$) compared with controls. Thereafter, this distance remained shorter than in controls into adulthood, with an average 4.87 mm (15%, $P = 0.043$) decrease overall. The horizontal projected length of pterion–FZR/L (the effective length of frontozygomatic suture in the Frankfort horizontal plane) was synchronously decreased, suggesting the more evidently limited horizontal growth of the frontozygomatic suture. This horizontal projected length was 4.46 mm (30%, $P = 0.004$) shorter than in controls before

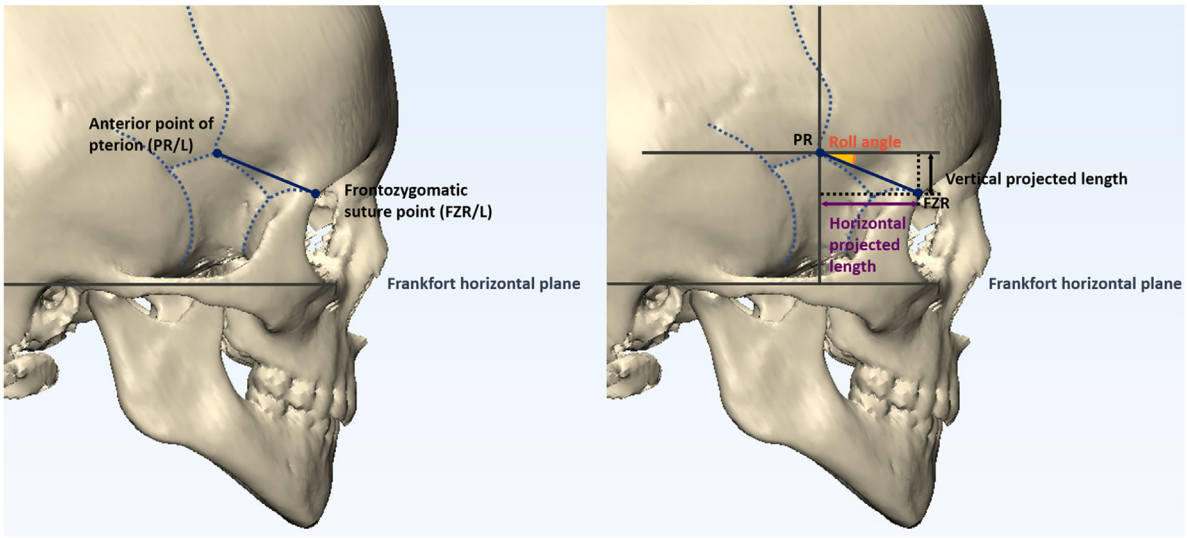

Fig. 3. The distance between the anterior point of pterion and the frontozygomatic suture point, indicating the frontozygomatic suture length (left). The horizontal and vertical projected lengths reflect the vector components. The roll angle is the angle between the line PR/L–FZR/L and the Frankfort horizontal plane.

Table 4. Age distribution of patients with Crouzon syndrome and controls.

Age group	Crouzon	Control	*P*-value
0–6 months			
Number	7	14	
Age (years)	0.19 ± 0.18	0.17 ± 0.13	0.76
Male/female	3/4	8/6	0.84
6 months–2 years			
Number	6	12	
Age (years)	0.96 ± 0.35	1.01 ± 0.30	0.77
Male/female	3/3	7/5	0.80
2–6 years			
Number	9	11	
Age (years)	4.51 ± 1.37	4.26 ± 1.58	0.72
Male/female	3/6	6/5	0.92
6–18 years			
Number	7	8	
Age (years)	12.16 ± 4.24	11.25 ± 4.78	0.70
Male/female	4/3	5/3	0.92
18–62 years			
Number	7	9	
Age (years)	36.86 ± 12.48	34.35 ± 12.00	0.70
Male/female	1/6	3/6	0.51
0–62 years			
Number	36	54	
Age (years)	10.84 ± 14.70	8.53 ± 13.22	0.45
Male/female	14/22	29/25	0.93

6 months of age, 6.98 mm (37%, $P = 0.002$) shorter between 6 months and 2 years, and remained shorter than controls into adulthood, with an average 5.84 mm (22%, $P < 0.001$) decrease overall. The vertical projected length of pterion–FZR/L was shorter, but this did not achieve statistical significance. The roll angle of frontozygomatic suture relative to the horizontal direction was increased 5.04° ($P < 0.001$) in Crouzon subjects when compared to control subjects, across all time points.

Geometry of zygoma

The fronto-orbital zygomatic angle (UORR/L–FZR/L–ORR/L) was larger before 6 months of age (21%, $P < 0.001$), normalized between 6 months and 2 years, and the difference re-emerged after 2 years. Crouzon zygomaticosphenoid angle (ZMR/L–FZR/L–ZTR/L) was more acute before 6 months of age (16%, $P < 0.001$), with an average angular decrease of 15% ($P < 0.001$) in all age groups (with the exception of a normalized angle from 6 months to 2 years of age). The frontal zygomatic angle (ZMR/L–ZPR/L–ZTR/L) was decreased between 6 months and 2 years (9%, $P = 0.017$), yet zygoma anterior angle (ZMR/L–ZPR/L–FZR/L) and zygoma vertical angle (FZR/L–ZPR/L–ZXR/L) overall, did not differ significantly (Fig. 7).

Midfacial measurements

The width of maxilla (ZMR–ZML) was greater by 24% on average in the Crouzon cohort, with a difference of 16% ($P = 0.024$) before age 6 months, reaching a peak of 31% ($P < 0.001$) at age 2 to 6 years. The Crouzon maxillary anteroposterior length (ANS–PP) was markedly decreased from 6 months to 2 years by 12% ($P < 0.001$), with an 8% ($P = 0.032$) reduction in whole group comparisons. The nasal base width (ALL–ALR) was wider in Crouzon subjects after 2 years ($P = 0.011$). The nasal length (N–Ro) of Crouzon subjects was only longer than controls prior to 6 months of age (20%, $P = 0.039$).

Discussion

The surgical treatment of Crouzon syndrome, following early cranioplasty, currently centers upon facial osteotomies such as Le Fort I, II, and III and midface distraction[13–18]. The ultimate purpose is to normalize the facial appearance of Crouzon syndrome patients in order to reduce potential future psychosocial problems. Thus, a comprehensive understanding of the anatomical deficits involved and their

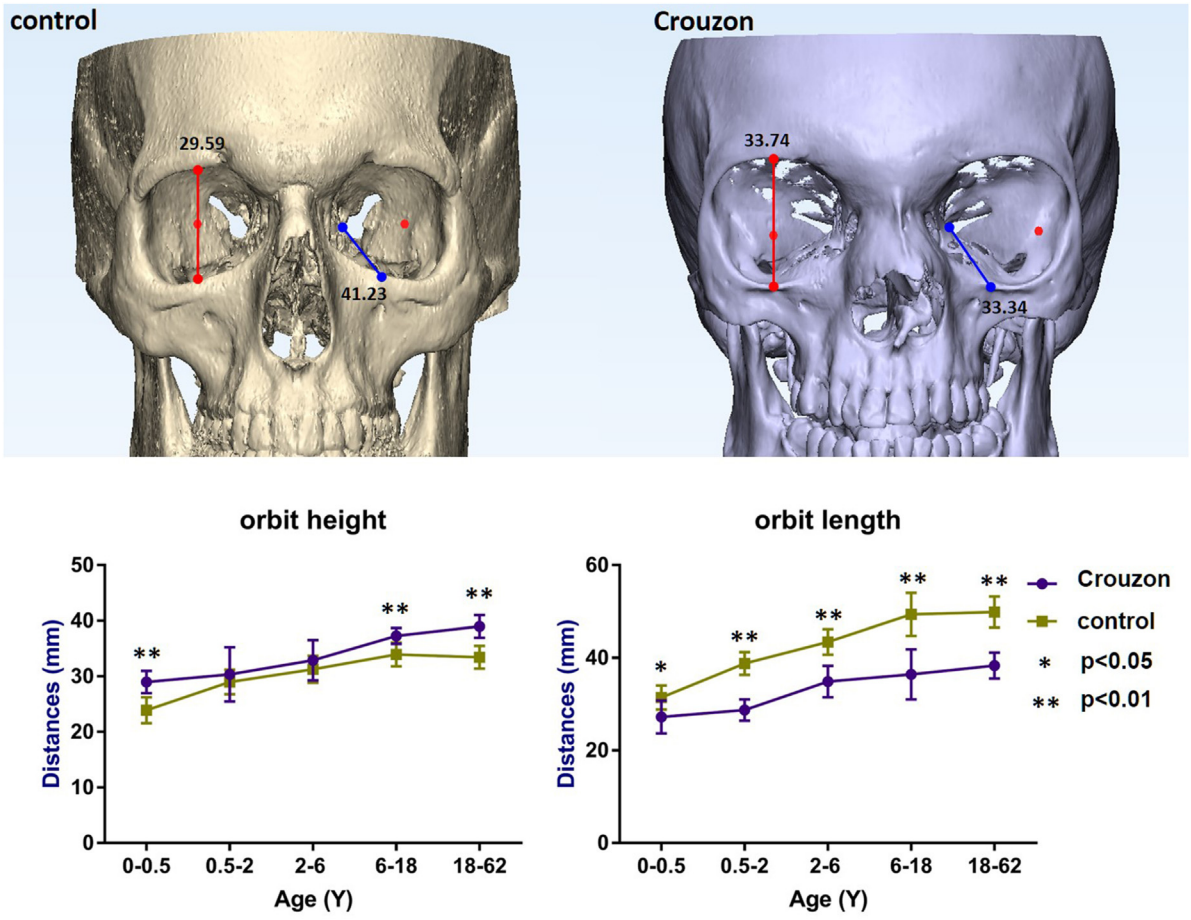

Fig. 4. Orbit height and length are shown on the CT scans of a 25-year-old female patient with Crouzon syndrome (right) and a control subject (left) as an example. Orbit length was defined as the distance from the zygomaticomaxillary suture on the orbital rim to the optic foramen. The distances marked are the average results for subjects aged 0 to 62 years. Red lines show that the distance was increased in Crouzon patients compared to control subjects and the blue lines show that the distance was decreased. The line charts show the changes according to age in the two groups.

evolution over time is critical in the choice of operation and the timing of procedures.

This study presents the largest known series of unoperated Crouzon patients undergoing anthropometric analysis. We previously found that the facial deformities in Crouzon syndrome develop synchronously with the deformities of cranial base, and mirror presumed local severity gradients[12]. Others have postulated that the earliest structural change is in the orbit and the most severe is in the midface[12]. The findings of the current study corroborate and support this hypothesis.

The first discrepancies to appear in the face were the shortened orbital floor length (presumably sphenoid bone) and the increased globe prominence, with a corresponding increase in the ratio of visual axis length to orbital depth. The magnitude of these differences increased with age. This parallels previous reports that have concluded that Crouzon syndrome patients have more severe and early ocular symptoms, such as corneal injury and hypoplasia[4,19]. In particular, the orbital depth is considered to be significantly influenced by the cranial anteroposterior and transverse diameters[20].

Increased orbital height also appeared early, but as an accompanying compensatory change (after shortening of anteroposterior length), when compared to controls aged 6 months to 6 years. The gap between Crouzon syndrome patients and the control subjects narrowed during childhood, likely due to the rapid growth of the normal orbit and proportionate greater growth than the maxilla, rather than the relief of orbital deformity in Crouzon syndrome. Chang et al. reported that, in general, the orbital depth in normal children increased rapidly before 6 years, but tended to stabilize at 10 years of age[20]. In the Crouzon patients in the present study, the orbital height increased at a constant rate until puberty. It is postulated that after 6 years of age, when the normal orbital growth rate begins to decline, compensatory growth continues and this gap re-emerges. Furthermore, the medial orbital width and the cornea position were noted postnatally, with differences persisting during development into adulthood. This is consistent with clinical observations and previous studies showing significant orbital widening[1,21].

Zygoma anterior protrusion was significantly decreased in early infancy, with a narrowing gap thereafter, yet no difference in the zygoma transverse width was seen. Considering the zygoma has a normal volume in Crouzon syndrome, the assumption is that the position of zygoma is the primary problem, with emphasis on the anteroposterior retropositioning. The decreased sphenofrontal suture length, especially its significantly shortened horizontal component, emphasizes the limited position of zygoma anteroposteriorly. The increased roll angle explains the minor shortening of its vertical component,

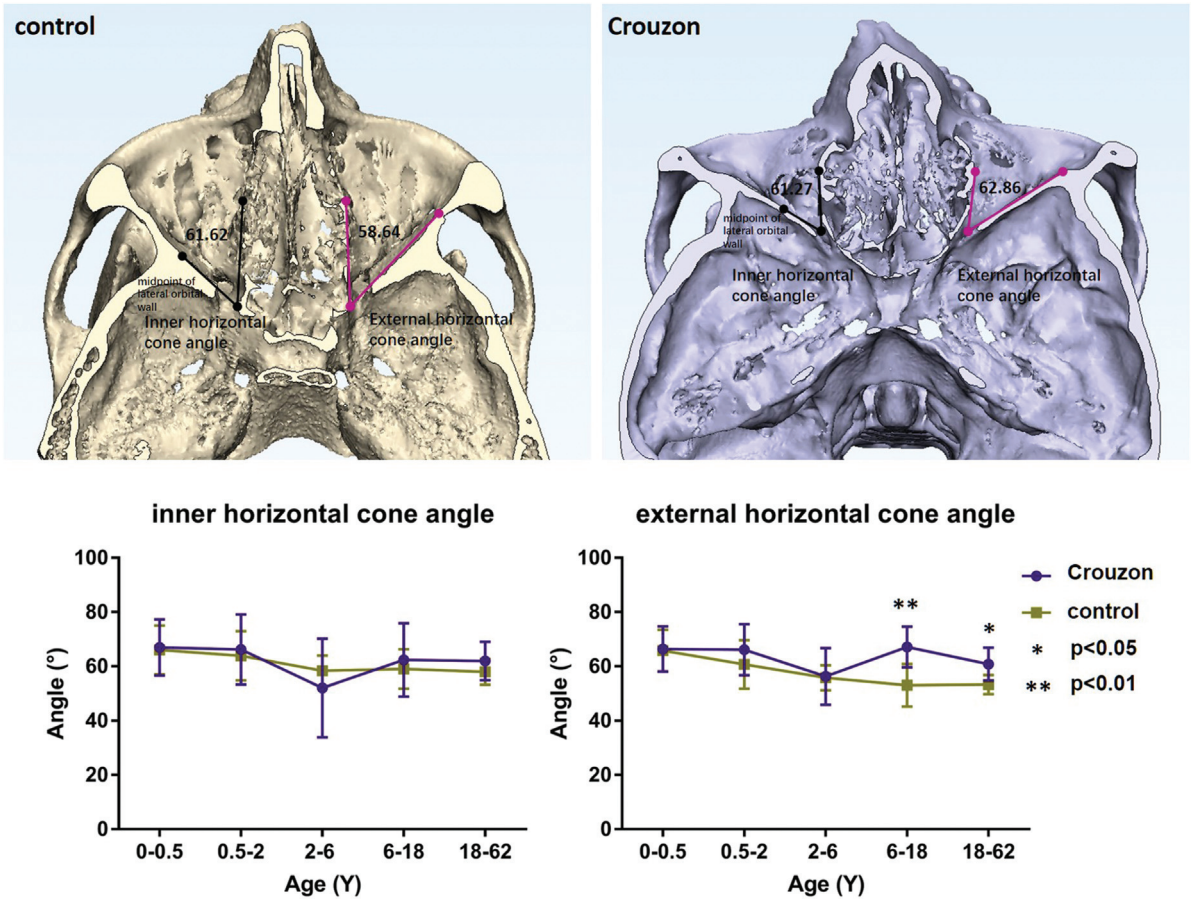

Fig. 5. The inner horizontal cone angle and external horizontal cone angle are shown on the CT scans of a 25-year-old female patient with Crouzon syndrome (right) and a control subject (left) as an example. The angles marked show the average size of these two angles, in degrees, for subjects aged 0 to 62 years. The inner horizontal cone angle did not differ between Crouzon patients and controls; however, the external horizontal cone angle was significantly increased in Crouzon patients. The line charts show the changes according to age in the two groups.

which may also be neutralized by the increased orbit height.

However, the data herein call into question the role of the maxilla. The maxilla, located at the base of the zygoma, was found to shorten significantly in the anteroposterior direction after 6 months of age. Zygoma retrusion, however, developed before 6 months. This suggests that the zygomatic-maxillary retrusion may be influenced independently, but in concert. As the growth of the vault is restricted in the direction perpendicular to the premature suture and premature cranial suture fusion impacts the cranial base before the midface[21–23], the zygoma is more likely to be affected by the premature coronal suture than the sphenozygomatic sutures. As the zygoma is connected to the vault through the temporal bone and the zygoma anteroposterior position is perpendicular to the coronal sutures, it is likely to have a relatively early impact, as the coronal sutures are the most frequently involved in Crouzon syndrome[24,25]. While the maxillary anteroposterior length is likely influenced by the deformed cranial base, and secondary growth disturbance may be induced by premature fusion of the coronal suture, the shortened maxillary length is a potentially tertiary effect. The locus of abnormal growth of the maxilla may be more central and inferior, such as in the greater wings of the sphenoid. This also suggests that the zygoma retrusion follows more closely the vault deformity, while the maxilla follows more closely cranial base malformation. Maxillary volume is normal in Crouzon syndrome[26], as is nasal height. This may reflect directionally consistent growth pattern influences.

Surprisingly, the maxilla widened before 6 months, but the sphenoid greater wing angle developed to be more obtuse in Crouzon syndrome afterwards and the pterygoid plates widened after 2 years of age. In the discussion of the interplay between sphenoid and maxilla, it is suspected that both the maxilla and the sphenoid mediolateral deformity are secondary effects after premature coronal suture. The maxilla likely follows the vault–zygoma–maxilla pathway, while the sphenoid likely follows the vault–cranial base pathway. Nevertheless, despite the knowledge that bone growth is typically influenced by adjacent structures, a causal relationship cannot be ascribed, and perhaps both structures have their internal developmental timelines.

While the skull base has been shown to regulate craniofacial development, there may be an alternative controller. Bones of the skull base, including the sphenoid, occipital, and petrous bones, arise from mesodermally derived ectomeninx, whereas facial bones, such as the zygoma, maxilla, and nasal bones, are formed from neural crest derivatives. Even the cranial base itself has a dual embryonic origin: the anterior base arises solely from the neural crest (and similar to the facial bones), while the posterior base arises from the paraxial mesoderm[27]. It is possible, then, that craniofacial development is governed by two different regulators, and both are controlled by the genetic abnormalities of Crouzon syndrome.

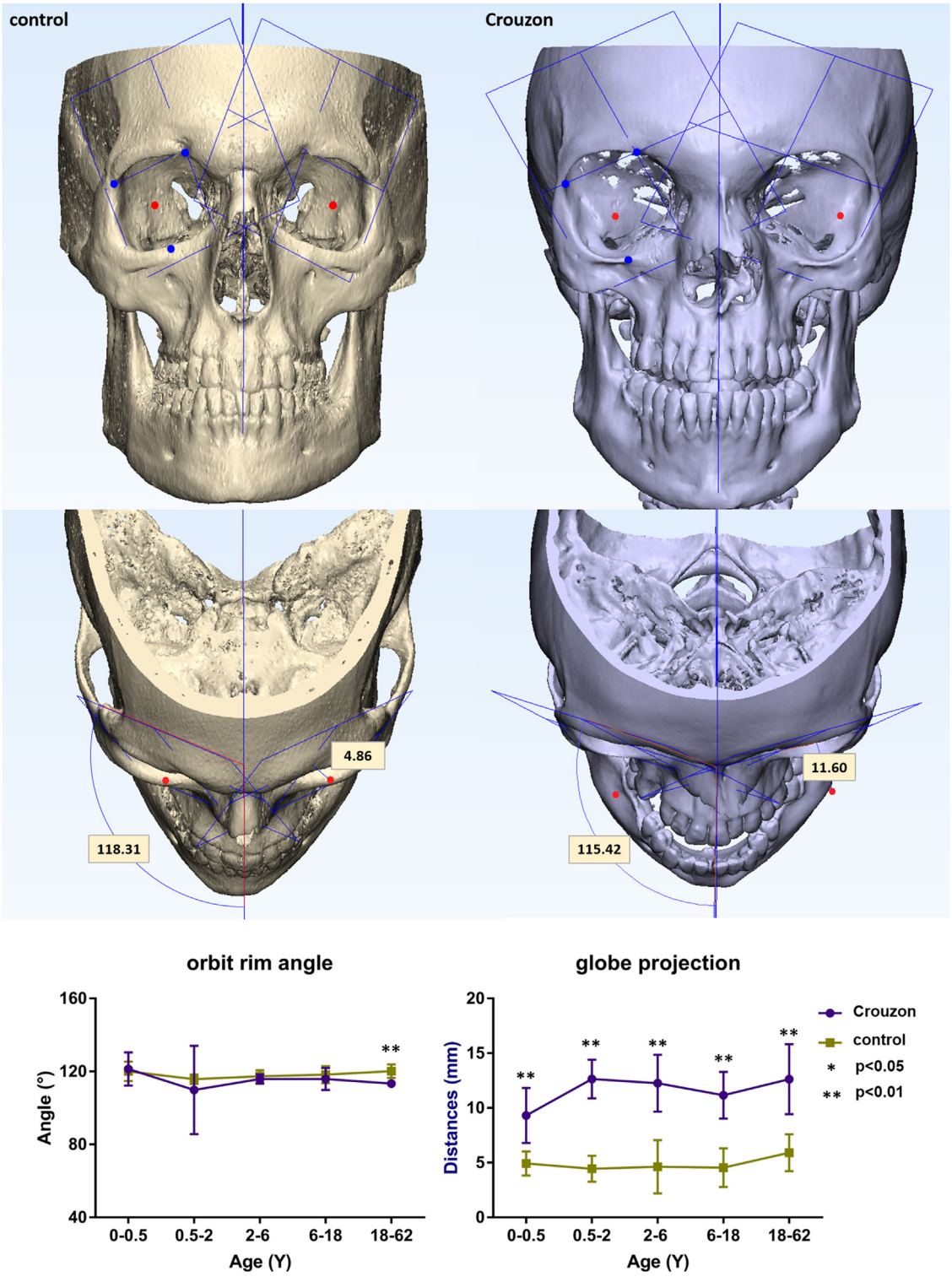

Fig. 6. The orbital rim angle and globe projection are shown on the CT scans of a 25-year-old female patient with Crouzon syndrome (right) and a control subject (left) as an example. The angles (degrees) and distances marked are the average results for all subjects aged 0–62 years. The line charts show the changes according to age in the two groups.

In addition, Crouzon syndrome is frequently associated with multiple premature suture synostoses and the most commonly affected are the coronal, sagittal, and lambdoid combined[24,25]. Sagittal synostosis, in particular, limits the transverse growth of the cranium and could limit the lateral position of zygoma. The coronal synostosis could limit the anteroposterior position of zygoma. Thus, individual midface differences may depend on the type of suture fusion rather than a global cranial base.

The position of zygoma and its relationship to the upper and lower face is a

Table 5. Orbit, zygoma, midface, and related cranial base measurements in the full age range (0–62 years) of Crouzon syndrome patients compared with controls.

Index	Crouzon		Control		*P*-value[a]	Change %
	Mean	SD	Mean	SD		
Orbit						
Unilateral orbital feature						
Orbit length	33.34	5.54	41.23	7.70	<0.001**	−19%
Orbit height	33.74	4.79	29.59	4.40	<0.001**	14%
Orbit width	33.67	4.96	31.94	4.51	0.098	5%
Vertical cone angle	60.19	5.94	54.31	3.69	<0.001**	11%
Inner horizontal cone angle	61.27	13.81	61.62	8.08	0.892	−1%
External horizontal cone angle	62.86	9.26	58.64	8.41	0.032*	7%
Orbital rim angle	115.42	10.94	118.31	4.32	0.139	−2%
Globe projection	11.60	2.68	4.86	1.67	<0.001**	139%
Visual axis length	43.86	5.27	42.63	6.61	0.332	3%
Visual axis length/orbital length	1.33	0.14	1.04	0.07	<0.001**	28%
Bilateral orbital relationship						
MOR–MOL	23.77	4.42	19.13	3.34	<0.001**	24%
FZR–FZL	88.31	13.21	80.89	12.06	0.009**	9%
UORR–UORL	59.20	9.61	48.00	7.89	<0.001**	23%
ORR–ORL	63.28	10.26	53.07	10.67	<0.001**	19%
OFR–OFL	25.17	5.83	22.63	5.11	0.037*	11%
Cornea R–Cornea L	64.63	9.26	52.57	8.01	<0.001**	23%
Bilateral optical axis angle	54.05	5.27	41.61	4.89	<0.001**	30%
Zygomatic linear measurements						
Zygoma anterior protrusion	18.42	5.85	11.79	2.64	<0.001**	56%
Zygoma self-protrusion	5.50	1.11	6.01	1.49	0.068	−8%
Zygoma height	33.97	9.24	32.95	8.69	0.604	3%
Zygoma length	36.76	7.71	40.57	8.74	0.037*	−9%
Zygoma superior curvature length	29.33	5.10	28.40	4.25	0.367	3%
Bizygomatic width	100.63	20.82	97.71	19.81	0.513	3%
Pterion–FZR/L	27.86	3.40	32.72	4.90	0.042*	−15%
Horizontal projected length of pterion–FZR/L	20.50	5.53	26.35	3.99	<0.001**	−22%
Rotated angle of pterion–FZR/L	38.47	13.25	33.43	5.21	<0.001**	15%
Geometry of zygoma						
UORR/L–FZR/L–ORR/L	92.47	6.40	81.97	6.18	<0.001**	13%
ZMR/L–FZR/L–ZTR/L	70.76	5.94	83.65	6.05	<0.001**	−15%
ZMR/L–ZPR/L–ZTR/L	126.57	8.51	128.89	7.86	0.201	−2%
ZMR/L–ZPR/L–FZR/L	83.19	20.25	82.82	19.28	0.932	0%
FZR/L–ZPR/L–ZXR/L	131.57	16.33	136.36	8.88	0.118	−4%
Midface						
ZMR–ZML	51.61	8.02	41.46	6.91	<0.001	24%
ANS–PP	46.13	7.93	50.26	9.84	0.032*	−8%
ALR–ALL	20.90	4.38	18.84	6.37	0.072	11%
NcR–NcL	24.11	5.65	21.55	3.54	0.019*	12%
N–Ro	16.55	7.52	15.55	5.45	0.495	6%
Ro–ANS	21.39	8.13	22.49	8.06	0.529	−5%
Related cranial base measurements						
Sphenoid greater wing angle	115.79	10.15	92.26	10.07	<0.001**	26%
PPR–S–PPL	72.38	6.68	65.83	6.18	<0.001**	10%
N–S–PP	80.48	7.37	76.85	4.29	0.011*	5%

SD, standard deviation.
[a] *P*-value, *t*-test: $*P < 0.05$; $**P < 0.01$.

significant consideration in guiding midface osteotomy and distraction. Therefore, in this study, the zygoma anterior protrusion was measured by the distance between the most anterior point of zygoma and the rear base plane, which passes through the midpoint of sella and is simultaneously perpendicular to the Frankfort horizontal plane and median sagittal plane. We did not use the relative distance to the frontal bone as in previous studies[28], because a special consideration in Crouzon syndrome patients is that there is often a deformity of the frontal bone itself as well[29].

Therefore, regarding the surgical intervention for Crouzon patients and considering the subtle changes that develop in orbit, zygoma, and maxilla, in addition to the initially macroscopic facial surgeries (Le Fort III and monobloc), subsequent precise extraction and other surgical procedures will be necessary at a later time in life in order to achieve an approximately normalized facial profile[30–32].

The limitation of this study is the relatively small number of adult patients and the large age range between them (i.e. 18 to 62 years of age). The inclusion criterion of this study was that the Crouzon patient must not have undergone any previous surgical intervention. Unoperated adult patients are very rare. The adult subgroup in this study

Table 6. Orbital measurement results shown by age subgroup; results are presented as the mean ± standard deviation value.

Index	0–6 months			6 months–2 years			2–6 years			6–18 years			18–62 years		
	Crouzon	Control	*P*-value[a]	Crouzon	Control	*P*-value[a]	Crouzon	Control	*P*-value[a]	Crouzon	Control	*P*-value[a]	Crouzon	Control	*P*-value[a]
Unilateral orbital features															
Orbit length	27.23 ± 3.55	31.43 ± 2.59	0.021*	28.74 ± 2.30	38.75 ± 2.46	<0.001**	34.89 ± 3.43	43.42 ± 2.77	<0.001**	36.41 ± 5.44	49.36 ± 4.64	<0.001**	38.34 ± 2.84	49.86 ± 3.34	<0.001**
Orbit height	28.96 ± 2.03	23.88 ± 2.35	<0.001**	30.36 ± 4.89	28.97 ± 2.22	0.533	32.89 ± 3.65	31.26 ± 2.44	0.269	37.25 ± 1.42	33.94 ± 2.11	0.0035**	38.99 ± 2.06	33.42 ± 2.07	<0.001**
Orbit width	26.45 ± 1.27	26.62 ± 1.81	0.796	31.80 ± 2.04	30.00 ± 1.60	0.094	33.37 ± 2.07	32.96 ± 2.02	0.664	37.44 ± 3.09	37.08 ± 2.24	0.804	39.11 ± 2.75	36.99 ± 2.22	0.125
Vertical cone angle	60.30 ± 6.68	55.03 ± 3.61	0.088	57.26 ± 4.60	55.85 ± 4.38	0.548	58.47 ± 3.85	53.04 ± 3.46	0.005**	64.47 ± 9.20	53.18 ± 3.42	0.017*	60.52 ± 2.19	53.67 ± 3.03	<0.001**
Inner horizontal cone angle	66.98 ± 10.32	66.03 ± 9.01	0.839	66.21 ± 12.90	63.88 ± 9.10	0.703	52.08 ± 18.20	58.41 ± 5.66	0.341	62.41 ± 13.52	59.03 ± 7.29	0.569	61.98 ± 7.13	57.96 ± 4.79	0.228
External horizontal cone angle	66.36 ± 8.37	65.77 ± 7.69	0.879	66.11 ± 9.41	60.67 ± 8.97	0.269	56.26 ± 10.44	55.82 ± 4.59	0.909	67.10 ± 7.54	53.05 ± 7.86	0.004**	60.83 ± 6.14	53.28 ± 3.47	0.017*
Orbital rim angle	121.36 ± 9.06	120.05 ± 5.33	0.733	109.86 ± 24.23	115.75 ± 2.63	0.578	115.81 ± 2.53	117.39 ± 3.38	0.249	115.85 ± 6.04	118.29 ± 4.77	0.406	113.34 ± 2.05	120.15 ± 3.68	<0.001**
Globe projection	9.31 ± 2.52	4.93 ± 1.11	0.003**	12.64 ± 1.76	4.44 ± 1.19	<0.001**	12.25 ± 2.60	4.62 ± 2.43	<0.001**	11.16 ± 2.14	4.54 ± 1.76	<0.001**	12.62 ± 3.21	5.91 ± 1.68	<0.001**
Visual axis length	36.59 ± 3.56	34.35 ± 2.38	0.168	41.14 ± 2.14	40.46 ± 2.20	0.542	44.85 ± 3.14	44.21 ± 2.71	0.634	46.29 ± 3.01	48.17 ± 3.25	0.264	49.74 ± 2.37	51.54 ± 2.21	0.146
Visual axis length/orbital length	1.36 ± 0.15	1.10 ± 0.06	0.003**	1.44 ± 0.12	1.05 ± 0.06	<0.001**	1.29 ± 0.13	1.02 ± 0.05	<0.001**	1.29 ± 0.14	0.98 ± 0.09	<0.001**	1.31 ± 0.13	1.04 ± 0.04	0.001**
Bilateral orbital relationship															
MOR–MOL	18.85 ± 1.91	16.71 ± 2.39	0.043*	20.45 ± 2.96	16.67 ± 1.31	0.024*	23.32 ± 2.48	19.66 ± 2.19	0.003**	27.90 ± 3.24	23.02 ± 1.96	0.006*	28.00 ± 1.98	22.08 ± 2.90	<0.001**
FZR–FZL	70.04 ± 2.46	67.88 ± 4.58	0.176	81.82 ± 7.75	74.49 ± 3.28	0.069	86.41 ± 2.95	82.49 ± 4.96	0.043*	99.86 ± 7.24	92.44 ± 6.03	0.054	103.05 ± 7.13	97.44 ± 7.00	0.139
UORR–UORL	48.13 ± 4.15	42.70 ± 3.63	0.014*	55.85 ± 10.19	45.49 ± 4.60	0.055	56.26 ± 3.41	47.26 ± 8.25	0.005**	65.85 ± 5.93	56.13 ± 6.97	0.012*	70.26 ± 4.75	53.29 ± 8.78	<0.001**
ORR–ORL	50.35 ± 4.17	44.89 ± 2.34	0.012*	60.13 ± 7.73	48.82 ± 3.62	0.014*	61.06 ± 5.96	53.83 ± 5.08	0.011*	71.79 ± 7.86	53.42 ± 14.05	0.009**	73.25 ± 4.93	70.21 ± 6.82	0.318
OFR–OFL	18.25 ± 1.56	17.36 ± 2.41	0.325	21.57 ± 1.16	19.87 ± 1.74	0.027*	23.10 ± 2.65	23.72 ± 2.30	0.589	31.98 ± 3.24	27.33 ± 4.25	0.033*	31.01 ± 2.42	28.99 ± 2.76	0.142
Cornea R–Cornea L	51.30 ± 4.63	44.92 ± 2.78	<0.001**	61.29 ± 3.94	47.17 ± 2.63	<0.001**	63.42 ± 2.59	53.07 ± 3.73	<0.001**	72.35 ± 5.34	61.20 ± 4.13	<0.001**	74.63 ± 4.69	63.40 ± 4.21	<0.001**
Bilateral optical axis angle	54.45 ± 8.91	47.44 ± 4.21	0.087	57.82 ± 2.90	39.62 ± 4.29	<0.001**	54.55 ± 2.67	38.77 ± 2.23	<0.001**	51.77 ± 5.47	41.25 ± 3.28	0.001**	52.06 ± 3.22	39.01 ± 2.11	<0.001**

[a] *P*-value: $*P < 0.05$; $**P < 0.01$.

Table 7. Zygoma, midface, and cranial base-related measurement results shown by age subgroup; results are presented as the mean ± standard deviation value.

Index	0–6 months			6 months–2 years			2–6 years			6–18 years			18–62 years		
	Crouzon	Control	*P*-value[a]	Crouzon	Control	*P*-value[a]	Crouzon	Control	*P*-value[a]	Crouzon	Control	*P*-value[a]	Crouzon	Control	*P*-value[a]
Zygomatic linear measurements															
Zygoma anterior protrusion	20.96 ± 4.67	10.27 ± 2.17	<0.001**	23.24 ± 7.23	13.08 ± 3.27	0.032*	16.69 ± 6.96	12.81 ± 2.53	0.144	18.01 ± 2.38	11.38 ± 1.93	<0.001**	15.07 ± 4.74	11.86 ± 2.38	0.138
Zygoma self-protrusion	4.93 ± 0.79	5.68 ± 1.71	0.189	5.93 ± 1.58	5.50 ± 0.45	0.578	4.79 ± 0.74	5.42 ± 0.67	0.064	5.66 ± 0.59	6.31 ± 1.53	0.291	6.50 ± 1.05	7.65 ± 1.71	0.123
Zygoma height	22.97 ± 2.59	22.25 ± 2.47	0.556	25.27 ± 2.71	29.65 ± 1.79	0.018*	33.27 ± 3.31	34.78 ± 3.00	0.305	43.54 ± 7.26	40.98 ± 4.59	0.441	42.52 ± 2.73	44.62 ± 4.22	0.249
Zygoma length	27.74 ± 2.78	30.34 ± 2.73	0.065	31.08 ± 3.53	37.51 ± 2.54	0.011*	36.58 ± 4.39	42.00 ± 3.21	0.008**	41.94 ± 5.82	49.19 ± 6.92	0.046*	44.89 ± 5.54	51.19 ± 5.37	0.040*
Zygoma superior curvature length	23.17 ± 2.07	23.10 ± 1.67	0.937	25.23 ± 3.54	27.39 ± 1.71	0.206	29.71 ± 3.78	29.38 ± 1.60	0.812	32.78 ± 0.92	33.26 ± 2.45	0.619	35.07 ± 1.90	32.46 ± 2.87	0.046*
Bizygomatic width	72.56 ± 6.65	74.54 ± 6.33	0.525	83.61 ± 5.82	87.57 ± 4.86	0.226	98.99 ± 5.18	101.68 ± 6.21	0.305	116.69 ± 6.74	119.11 ± 10.48	0.600	126.90 ± 6.17	123.42 ± 6.52	0.293
Pterion–FZR/L	14.72 ± 2.85	18.34 ± 2.97	0.018*	20.40 ± 2.34	23.80 ± 2.35	0.013*	23.00 ± 1.59	26.25 ± 1.81	<0.001**	29.10 ± 3.54	32.14 ± 4.41	0.1825	26.61 ± 2.97	33.18 ± 5.47	0.009**
Projected length of pterion–FZR/L	10.48 ± 2.66	14.94 ± 2.77	0.004**	11.80 ± 3.23	18.77 ± 1.77	0.002**	15.60 ± 4.46	21.31 ± 2.26	0.005**	21.92 ± 4.26	25.52 ± 4.34	0.144	19.09 ± 6.60	27.00 ± 3.82	0.020*
Rotated angle of pterion–FZR/L	32.82 ± 8.05	25.44 ± 9.49	0.083	41.71 ± 9.25	29.99 ± 5.20	0.025*	38.61 ± 14.15	29.40 ± 5.09	0.096	35.97 ± 8.26	33.24 ± 5.04	0.472	40.97 ± 17.26	33.58 ± 5.64	0.313
Geometry of zygoma															
UORR/L–FZR/L–ORR/L	96.59 ± 5.81	79.56 ± 5.89	<0.001**	93.02 ± 7.63	85.07 ± 4.84	0.0795	90.02 ± 7.58	80.74 ± 7.52	0.014*	91.07 ± 4.17	80.55 ± 6.13	0.002**	92.54 ± 5.82	84.36 ± 5.06	0.012*
ZMR/L–FZR/L–ZTR/L	68.46 ± 2.69	81.67 ± 4.08	<0.001**	76.55 ± 5.74	82.57 ± 5.96	0.088	69.59 ± 4.24	82.12 ± 4.93	<0.001**	71.95 ± 6.68	84.44 ± 7.70	0.005**	69.23 ± 7.83	89.33 ± 5.99	<0.001**
ZMR/L–ZPR/L–ZTR/L	119.88 ± 9.06	121.79 ± 3.94	0.611	119.61 ± 7.21	131.29 ± 5.68	0.017*	131.09 ± 8.59	133.72 ± 5.42	0.439	131.79 ± 3.62	134.61 ± 7.62	0.372	127.22 ± 5.12	125.74 ± 8.92	0.684
ZMR/L–ZPR/L–FZR/L	102.66 ± 7.47	102.88 ± 3.97	0.941	96.82 ± 13.71	91.60 ± 11.05	0.477	88.57 ± 17.88	77.98 ± 18.52	0.212	65.26 ± 13.69	66.93 ± 10.68	0.799	65.00 ± 11.31	59.95 ± 6.96	0.325
FZR/L–ZPR/L–ZXR/L	134.27 ± 6.41	129.67 ± 4.59	0.124	132.21 ± 12.21	136.47 ± 9.53	0.511	140.13 ± 9.89	140.97 ± 7.25	0.835	125.70 ± 21.90	145.06 ± 6.55	0.059	123.29 ± 22.83	133.28 ± 8.14	0.305
Midface															
ZMR–ZML	40.95 ± 4.80	35.45 ± 3.56	0.024*	48.23 ± 3.57	36.90 ± 3.38	<0.001**	51.39 ± 4.11	43.13 ± 4.94	<0.001**	55.79 ± 6.51	47.39 ± 6.28	0.025*	61.28 ± 1.84	49.58 ± 2.67	<0.001**
ANS–PP	37.22 ± 3.68	38.97 ± 2.24	0.279	39.43 ± 1.57	45.00 ± 2.03	<0.001**	45.57 ± 3.58	52.29 ± 3.56	<0.001**	53.92 ± 7.42	62.15 ± 5.35	0.034*	52.77 ± 3.99	61.77 ± 5.15	0.002**
ALR–ALL	15.18 ± 2.28	15.03 ± 1.52	0.876	17.68 ± 1.11	16.73 ± 1.18	0.120	20.91 ± 2.28	18.36 ± 1.22	0.011*	24.86 ± 1.76	25.76 ± 13.57	0.858	25.43 ± 2.24	22.05 ± 2.83	0.019*
NcR–NcL	16.95 ± 3.17	17.74 ± 1.47	0.548	19.14 ± 3.34	20.46 ± 1.42	0.390	24.74 ± 2.43	22.72 ± 2.45	0.084	29.14 ± 2.27	24.85 ± 3.30	0.012*	29.70 ± 1.64	24.55 ± 3.13	0.001**
N–Ro	11.89 ± 1.94	9.94 ± 0.90	0.039*	13.57 ± 1.47	13.10 ± 1.55	0.545	12.02 ± 8.60	16.22 ± 3.14	0.195	23.40 ± 3.82	19.53 ± 5.85	0.150	22.72 ± 6.87	23.16 ± 2.06	0.876
Ro–ANS	14.96 ± 1.57	15.45 ± 1.63	0.512	19.15 ± 4.69	20.93 ± 11.79	0.655	19.27 ± 12.62	22.75 ± 2.96	0.439	26.88 ± 3.36	27.82 ± 3.07	0.587	26.97 ± 3.05	30.47 ± 5.05	0.110
Related cranial base measurements															
Sphenoid greater wing angle	114.64 ± 14.64	103.03 ± 7.66	0.086	117.07 ± 14.16	89.98 ± 10.12	0.003**	113.82 ± 5.90	91.38 ± 7.20	<0.001**	118.52 ± 9.07	86.17 ± 4.65	<0.001**	115.65 ± 8.57	85.01 ± 6.58	<0.001**
PPR–S–PPL	71.17 ± 4.58	71.86 ± 4.80	0.752	69.17 ± 6.30	62.35 ± 4.25	0.072	74.92 ± 7.45	63.81 ± 4.62	0.002**	74.37 ± 7.67	61.78 ± 5.65	0.004**	70.63 ± 6.64	67.16 ± 5.53	0.288
N–S–PP	78.29 ± 6.35	76.40 ± 3.68	0.489	71.01 ± 5.26	74.52 ± 4.57	0.237	80.85 ± 5.22	76.30 ± 3.38	0.042*	87.61 ± 5.94	79.46 ± 5.22	0.016*	81.83 ± 5.96	78.99 ± 3.52	0.290

[a] *P*-value: $*P < 0.05$; $**P < 0.01$.

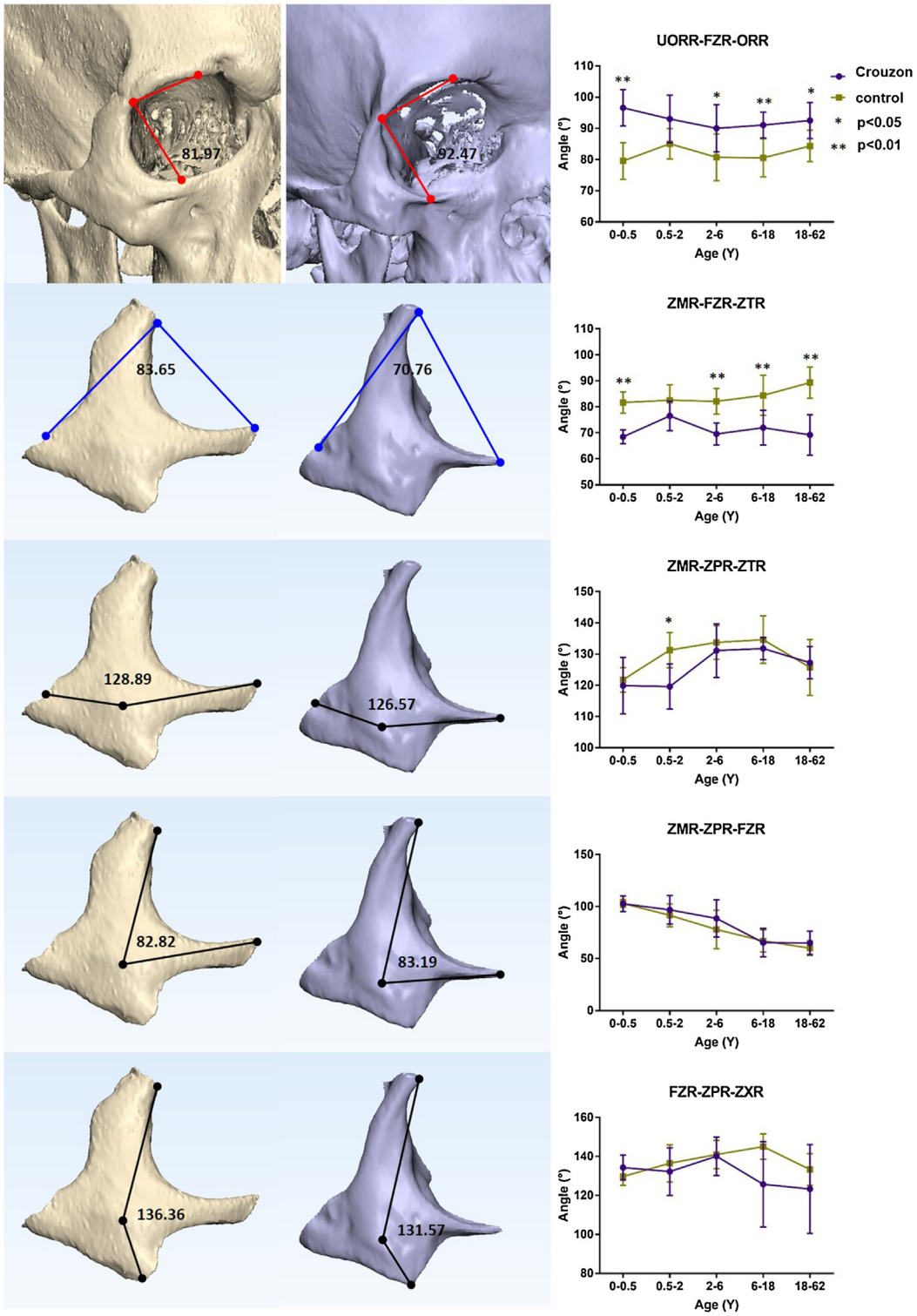

Fig. 7. Geometric angles of zygoma are shown on the CT scans of a 25-year-old female patient with Crouzon syndrome (right) and a control subject (left) as an example. The angles (degrees) and distances marked are the average results for all subjects aged 0–62 years. Red lines show that the angle was increased in Crouzon patients compared to controls, blue lines show the angle was decreased in Crouzon patients compared to controls, and the black lines show angles that did not differ between Crouzon patients and controls. The line charts show the changes according to age in the two groups.

consisted of seven patients, which is likely one of the largest unoperated adult Crouzon groups reported; yet they may have had individual variations. The predominance of female Crouzon subjects is consistent with the sex distribution of Crouzon syndrome. Sex-matched controls were included in each age subgroup to counteract the potential influencing factors caused by sex.

In summary, the orbit, zygoma, and maxilla in Crouzon syndrome form a complete anatomical region, but each has its individual developmental features. The high and shallow orbital walls are distinctive. The anteroposterior position of zygoma is likely a principal deformity, rather than the intrinsic distortion of the shape of the bone. Maxillary widening developed before the malformation of sphenoid, which suggests a dual-thread regulatory mechanism from the premature coronal suture, influencing zygoma development, which then in turn influences maxillary movement.

Funding

None.

Competing interests

None.

Ethical approval

Yale University Human Investigation Committee (HIC 1101007932).

Patient consent

Not required.

References

1. Carr M, Posnick JC, Pron G, Armstrong D. Cranio-orbito-zygomatic measurements from standard CT scans in unoperated Crouzon and Apert infants: comparison with normal controls. *Cleft Palate Craniofac J* 1992;**29**:129–36.
2. Enlow DH. A morphogenetic analysis of facial growth. *Am J Orthod* 1966;**52**:283–99.
3. Waitzman AA, Posnick JC, Armstrong DC, Pron GE. Craniofacial skeletal measurements based on computed tomography: Part II. Normal values and growth trends. *Cleft Palate Craniofac J* 1992;**29**:118–28.
4. Balyen L, Deniz Balyen LS, Pasa S. Clinical characteristics of Crouzon syndrome. *Oman J Ophthalmol* 2017;**10**:120–2.
5. Gray TL, Casey T, Selva D, Anderson PJ, David DJ. Ophthalmic sequelae of Crouzon syndrome. *Ophthalmology* 2005;**112**:1129–34.
6. Coll G, Arnaud E, Collet C, Brunelle F, Sainte-Rose C, Di Rocco F. Skull base morphology in fibroblast growth factor receptor type 2-related faciocraniosynostosis: a descriptive analysis. *Neurosurgery* 2015;**76**:571–83. discussion 583.
7. Kreiborg S, Cohen Jr MM. Ocular manifestations of Apert and Crouzon syndromes: qualitative and quantitative findings. *J Craniofac Surg* 2010;**21**:1354–7.
8. Forte AJ, Steinbacher DM, Persing JA, Brooks ED, Andrew TW, Alonso N. Orbital dysmorphology in untreated children with Crouzon and Apert syndromes. *Plast Reconstr Surg* 2015;**136**:1054–62.
9. Imai K, Fujimoto T, Takahashi M, Maruyama Y, Yamaguchi K. Preoperative and postoperative orbital volume in patients with Crouzon and Apert syndrome. *J Craniofac Surg* 2013;**24**:191–4.
10. Kang M. Three-dimensional approach to zygoma reduction: review of 221 patients over 7 years. *Ann Plast Surg* 2016;**76**:51–6.
11. Williams SE, Slice DE. Influence of edentulism on human orbit and zygomatic arch shape. *Clin Anat* 2014;**27**:408–16.
12. Lu XN, Forte AJ, Sawh-Martinez R, Madari S, Wu R, Cabrejo R, Steinbacher DM, Alperovich M, Alonso N, Persing JA. Facial malformation in Crouzon's syndrome is consistent with cranial base development in time and space. *Plast Reconstr Surg Glob Open* 2018;**6**:e1963.
13. id="sbref0065">Kuroda S, Watanabe K, Ishimoto K, Nakanishi H, Moriyama K, Tanaka E. Long-term stability of LeFort III distraction osteogenesis with a rigid external distraction device in a patient with Crouzon syndrome. *Am J Orthod Dentofacial Orthop* 2011;**140**:550–61.
14. Nout E, Cesteleyn LL, van der Wal KG, van Adrichem LN, Mathijssen IM, Wolvius EB. Advancement of the midface, from conventional Le Fort III osteotomy to Le Fort III distraction: review of the literature. *Int J Oral Maxillofac Surg* 2008;**37**:781–9.
15. Komuro Y, Shimizu A, Ueda A, Miyajima M, Nakanishi H, Arai H. Whole cranial vault expansion by continual occipital and fronto-orbital distraction in syndromic craniosynostosis. *J Craniofac Surg* 2011;**22**:269–72.
16. Tay YC, Tan KH, Yeow VK. High Le Fort I and bilateral split sagittal osteotomy in Crouzon syndrome. *J Craniofac Surg* 2013;**24**:e253–5.
17. Wiltfang J, Hirschfelder U, Neukam FW, Kessler P. Long-term results of distraction osteogenesis of the maxilla and midface. *Br J Oral Maxillofac Surg* 2002;**40**:473–9.
18. Hopper RA, Kapadia H, Susarla SM. Le Fort II distraction with zygomatic repositioning: a technique for differential correction of midface hypoplasia. *J Oral Maxillofac Surg* 2018;**76**. 2002.e1–2002.e14.
19. Weiss AH, Kelly JP, Hopper RA, Phillips JO. Crouzon syndrome: relationship of eye movements to pattern strabismus. *Invest Ophthalmol Vis Sci* 2015;**56**:4394–402.
20. Chang JT, Morrison CS, Styczynski JR, Mehan W, Sullivan SR, Taylor HO. Pediatric orbital depth and growth: a radiographic analysis. *J Craniofac Surg* 2015;**26**:1988–91.
21. Rosenberg P, Arlis HR, Haworth RD, Heier L, Hoffman L, LaTrenta G. The role of the cranial base in facial growth: experimental craniofacial synostosis in the rabbit. *Plast Reconstr Surg* 1997;**99**:1396–407.
22. Babler WJ, Persing JA, Winn HR, Jane JA, Rodeheaver GT. Compensatory growth following premature closure of the coronal suture in rabbits. *J Neurosurg* 1982;**57**:535–42.
23. Babler WJ, Persing JA. Experimental alteration of cranial suture growth: effects on the neurocranium, basicranium, and midface. *Prog Clin Biol Res* 1982;**101**:333–45.
24. Goldberg JS, Enlow DH, Whitaker LA, Zins JE, Kurihara S. Some anatomical characteristics in several craniofacial syndromes. *J Oral Surg* 1981;**39**:489–98.
25. Kreiborg S. Crouzon syndrome. A clinical and roentgencephalometric study. *Scand J Plast Reconstr Surg Suppl* 1981;**18**:1–198.
26. Forte AJ, Alonso N, Persing JA, Pfaff MJ, Brooks ED, Steinbacher DM. Analysis of midface retrusion in Crouzon and Apert syndromes. *Plast Reconstr Surg* 2014;**134**:285–93.
27. Nie X. Cranial base in craniofacial development: developmental features, influence on facial growth, anomaly, and molecular basis. *Acta Odontol Scand* 2005;**63**:127–35.
28. Pfaff MJ, Wong K, Persing JA, Steinbacher DM. Zygomatic dysmorphology in unicoronal synostosis. *J Plast Reconstr Aesthet Surg* 2013;**66**:1096–102.
29. Burdi AR, Kusnetz AB, Venes JL, Gebarski SS. The natural history and pathogenesis of the cranial coronal ring articulations: implications in understanding the pathogenesis of the Crouzon craniostenotic defects. *Cleft Palate J* 1986;**23**:28–39.
30. Nishimoto S, Oyama T, Nagashima T, Osaki Y, Yoshimura Y, Fukuda K, Kawai K, Tsumano T, Kakibuchi M. Lateral orbital expansion and gradual fronto-orbital advancement: an option to treat severe syndromic craniosynostosis. *J Craniofac Surg* 2008;**19**:1622–7.
31. Laure B, Moret A, Joly A, Travers N, Listrat A, Krastinova D, Goga D. Orbitofrontal monobloc advancement for Crouzon syndrome. *J Craniomaxillofac Surg* 2014;**42**:e335–8.
32. Ko EW, Chen PK, Tai IC, Huang CS. Fronto-facial monobloc distraction in syndromic craniosynostosis. Three-dimensional evaluation of treatment outcome and facial growth. *Int J Oral Maxillofac Surg* 2012;**41**:20–7.

Address:
John A. Persing
Section of Plastic and Reconstructive Surgery
Yale School of Medicine
330 Cedar Street
3rd floor Boardman Building
New Haven
CT 06520
USA
E-mail: john.persing@yale.edu